Available online at www.sciencedirect.com
ScienceDirect
Catalysis Today 120 (2007) 383–388
CATALYSIS TODAY
www.elsevier.com/locate/cattod

A theoretical study of activated nanostructured materials for hydrogen storage

Seung-Hoon Jhi *

Department of Physics, POSTECH, San 31, Hyoja-Dong, Pohang 790-784, Republic of Korea

Available online 7 November 2006

Abstract

The adsorption of molecular hydrogen on activated nanostruture materials is studied through computational simulations based on the pseudopotential density functional method. The hydrogen sorption energy and its diffusion through chemically activated pores in the materials are particularly investigated. It is found that the sorption energy of hydrogen reaches as high as about 29 kJ/mol at activated sites and can be controlled by modifying the structure and chemistry of the pores. The equilibrium pressure of hydrogen adsorption is also presented as a function of temperature by including the temperature and pressure dependence of hydrogen entropy. The desorption temperature is estimated to be close to 270 K for optimized activated nanostructures. This study demonstrates a pathway of materials search based on computational simulations for proper media that can hold hydrogen at ambient conditions through physisorption.
© 2006 Elsevier B.V. All rights reserved.

Keywords: Activated nanotubes; Hydrogen adsorption; Simulations; Physisorption

1. Introduction

Hydrogen is considered as an ideal material for alternative energy source [1–3]. One of the major problems faced by the hydrogen economy is the lack of proper storage media of hydrogen. Compressed gas or liquid hydrogen are currently being used in prototype hydrogen-fueled vehicles, but they inherently have serious technical drawbacks such as bulky tank size, safety problems, and extra energy cost for liquidation, which should be critical issues for commercial hydrogen storages. There have been attempts to store hydrogen in solid phase storages or in new forms of materials such as metal hydrides, carbon nanotubes, and chemical hydrides [1], but none of them has yet achieved both goals of high hydrogen capacity and moderate desorption temperature set by the US DOE. More robust and systematic approaches in searching for hydrogen storage media are needed, and the atomistic understanding of hydrogen sorption on materials is believed to constitute a key component in such processes.

The adsorption of molecular hydrogen on surfaces is in nature a type of physisorption due to strong H–H bond and closed-shell electronic configuration of the molecule. The binding energy of H_2 on solid surface is thus usually very small. For example, the binding energy of hydrogen on graphite or carbon nanotubes is about 6 kJ/mol which inevitably leads to very high pressure (several hundred bars) and/or very low temperature (~77 K) to store meaningful amount of hydrogen in these materials. As the strength of the interaction between hydrogen and adsorbent materials increases, molecular hydrogen tends to dissociate into atomic hydrogen and subsequently diffuse into the adsorbents, which is typically observed in metal hydrides. The heat of adsorption then increases so significantly to more than 100 kJ/mol that the release of hydrogen should occur at very high temperatures. The desorption temperature (T_D) reaches about 300 °C for MgH_2, for example. The energy scale involved in storing hydrogen differs significantly for those two processes, and unfortunately there are no methods or theories known capable to continuously control the strength of hydrogen binding to materials, for example, from physisorption to chemisorption energies. Modifying chemistry or structures of materials that can hold hydrogen in either atomic or molecular form is a feasible way to change desorption temperature though in a limited range. A question is how we choose right materials and efficiently perform optimal modifications. There have been several attempts to increase T_D in carbon-based materials by mixing a small amount of

* Tel.: +82 54 279 2094; fax: +82 54 279 3099.
E-mail address: jhish@postech.ac.kr.

0920-5861/$ – see front matter © 2006 Elsevier B.V. All rights reserved.
doi:10.1016/j.cattod.2006.09.025

alkali or transition metals [4]. The metal atoms, however, simultaneously increase the mass-density of adsorbent material, and thus only limited quantities of metals can be added without sacrificing the hydrogen capacity. In this paper, we present an example of heuristic but systematic approaches based on quantum mechanical atomistic calculations to improve the sorption strength of molecular hydrogen on nanostructured materials.

The capacity of a hydrogen storage material through physisorption is limited by its specific surface area (SSA) [5–7], and the desorption (or release) temperature of hydrogen is determined by the strength of the interaction between hydrogen and the material's surface, called the heat of adsorption. A straightforward way to estimate the heat of adsorption is to calculate the binding energy of hydrogen on the surface of the material. These two parameters would be better to be treated separately so that the search for hydrogen storages can be pursued in parallel to reach both the goals of the storage capacity and operation temperature. Materials search by computations for room temperature hydrogen storages first focuses on finding proper materials that have a hydrogen binding energy of about 20–30 kJ/mol as estimated by the van't Hoff equation [8]. Developing optimized structures with large surface area for the computationally screened materials is the next step to follow.

The surface area of about 1000 m^2/g or higher is a big constraint in the search for hydrogen storage based on physisorption. Materials made of the first row elements would be a natural choice, and their nanostructured forms are expected to provide several advantages such as high surface area and relatively strong chemical reactivity with respect to hydrogen adsorption. Recently, Jhi et al. showed that non-carbon light-element nanostructured compounds could be potential hydrogen storages with higher desorption temperatures than carbon-based materials [9–11]. Here we choose two types of nanotubes to study the effect of chemical activation on hydrogen adsorption, namely boron nitride nanotubes (BNTs) and carbon nanotubes (CNTs). The BNTs have sp^2-like bonding as carbon nanotubes and thus are expected to have high surface area. Previous studies also showed that hydrogen molecules bind more strongly on BNT than on CNT [10]. An interesting feature of BNTs is that they have substantial buckling of B–N bonds and hence a dipole layer of boron atom and nitrogen atom shells [12,13]. The dipole shell may induce extra dipole moment in hydrogen, leading to a stronger adsorption of hydrogen. This feature may in fact be true for all ionic materials because the (induced) dipole moment of hydrogen is sensitive to local electric fields. While atomic substitution in hexagonal boron nitride (hBN) was shown to increase the chemical reactivity and hydrogen binding strength, there have been few systematic and atomistic studies on how chemical activations in nanotubes can affect the adsorption of hydrogen. It is also interesting to compare the effects of the activation in different platforms of nanotubes.

2. Computational methods

In order to estimate the heat of adsorption of hydrogen on candidate materials, a series of total energy calculations based on *ab initio* pseudopotential density functional methods were performed [14]. Computation by these methods can predict key physical properties of materials such as crystal structure, electronic and optical properties, transport properties, and gas adsorption kinetics. Atomic orbitals with double-ζ polarization are used for the expansion of single-particle wavefunctions with a cut-off energy of 80 Ry for real-space mesh construction [15]. We choose 0.01 Ry for the confinement energy shift, which defines the cut-off radii of the atomic orbitals. The exchange-correlation interaction of electrons is treated with a generalized gradient approximation approach (GGA) [16], which is known to be superior to the local density approximation (LDA) and has been successful in describing a wide range of interactions. At each step of the total energy calculations, a full range of structural relaxation is carried out under the constraint of a fixed distance between H_2 and adsorbents until their Hellmann–Feynman forces are less than 0.01 eV/Å. Once a set of values for the total energy as a function of the distance between H_2 and adsorbents has been calculated, the data are fit with Morse function. The minimum total energy corresponding to the heat of adsorption and the binding distance, at which the minimum occurs, are then obtained.

Once the binding energy is obtained, the desorption temperature and equilibrium pressure of hydrogen can be estimated from a thermodynamic equation known as the van't Hoff equation [8]. For a more accurate estimation, we need to know the entropy of hydrogen at gas and adsorbed phase, respectively, at varying temperature and pressure. We assume that the entropy of adsorbed hydrogen can be approximated as that of liquid hydrogen and is not sensitive to temperature and pressure. The temperature (T) and pressure (p) dependence of entropy of hydrogen gas was fully considered by fitting the experimental data [17] to a simple ideal gas-like form,

$$\Delta S(p,T) = S_0 + a_p \log(p) + a_T \log(T), \quad (1)$$

where S_0, a_p, and a_T are fitting parameters. The equilibrium pressure of hydrogen is plotted in Fig. 1 as a function of temperature for several hydrogen binding energies. The desorption temperature, which is defined as the temperature that gives the equilibrium pressure of 1 atm (or more precisely 1 bar), can reach as high as 270 K when the binding energy is about 30 kJ/mol. We note that the pressure of hydrogen should go over several hundred bars if we use activated carbons to store hydrogen at room temperature.

3. Results and discussion

3.1. Atomic substitution

As a starting template, a perfect (10,0) BNT is chosen for studying the hydrogen adsorption. First, some aspects of hydrogen binding on the perfect heteropolar nanotube are briefly given [10], and then the effect of atomic defects in the nanotube will be discussed. Fig. 2 shows schematic views of boron nitride nanotubes with: (a) substitutional atomic doping, (b) 5 × 7 Stone–Wales defect pair, and (c) a hydrogen molecule on top of the atomic defect. For computation of hydrogen

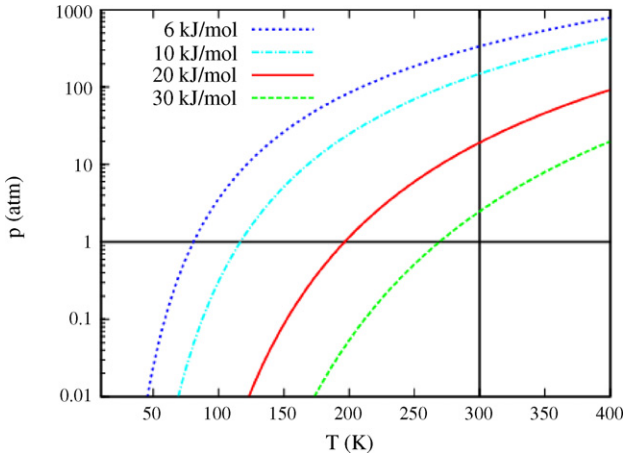

Fig. 1. Equilibrium pressures (in atmospheric pressure unit) of hydrogen adsorption on surfaces are plotted as a function of temperature using van't Hoff equation for several binding energies. The entropy change (ΔS in Eq. [8]) is estimated by subtracting the entropy in liquid phase from that in gas phase at given temperature and pressure, which is in turn obtained by fitting the measured data from the literature [17]. The desorption temperature reaches as high as 270 K when the binding energy is about 30 kJ/mol. For activated carbons, the binding energy is about 6 kJ/mol and it needs a pressure of several hundred atmospheric pressure for the full capacity adsorption of hydrogen at near room temperature.

binding on BNT, the nanotubes are put in a supercell of triangular lattice with 25 Å tube–tube distance. The wall-to-wall distance is 17 Å for (10,0) tubes, which is enough to minimize the effect from adjacent tubes on hydrogen binding. The H_2–H_2 distance along the tube axis is about 8.6 Å, and the intermolecular interaction can be neglected. It is found that nitrogen atoms move outward by 0.05 Å from boron atom layer, creating boron and nitrogen dipole shells. Fig. 3 shows the calculated binding energy curves of hydrogen on: (a) a perfect and (b) a carbon-doped (10,0) boron nitride nanotube (details are given below). The difference between the minimum total energy and that at 7 Å is defined as the binding energy. For the perfect BNT, the binding is the biggest for hydrogen on top of the center of hexagon rings, but the difference in energy between sites is not significant. Compared to carbon nanotubes (∼6 kJ/mol [18–21]), perfect BNTs have about 40% larger binding energy, and the desorption temperature is estimated to be about 125 K, well above the liquid nitrogen temperature. Although T_D is still much lower than the room temperature, it would be of significant importance to be above the liquid nitrogen temperature for practical applications. In fact, recent studies by Ma et al. [22,23] showed that boron nitride nanotube can adsorb hydrogen up to 2.6 wt% at about 10 MPa at room temperature, which is larger in capacity than multiwall carbon nanotubes. The nanotubes in that study have bamboo-like structures and their surface area is not significant (about 200 m^2/g) compared to that of high surface area activated carbon (∼2600 m^2/g) [24]. Since the capacity of hydrogen storage depends on the surface area, the study demonstrated that BNT can be a good hydrogen storage material once high surface area is achieved, which is in accord with the present calculations. Synthesis of high surface area BNT at large quantities is required for enhancing the capacity and also for future applications [25].

Next, we consider atomic substitutions in BNT to study the effect of atomistic chemical modifications on hydrogen binding. First we substitute a boron or nitrogen atom in BNT by a carbon atom, which can readily form sp^2-like bonding with surrounding B or N atoms. It is well known that the BNT can retain the sp^2-like bonding and hence the tubular structure even if a substantial amount of boron and nitrogen atoms are replaced by carbon. For example, it is possible to control the chemical composition in $B_xC_yN_z$ while maintaining

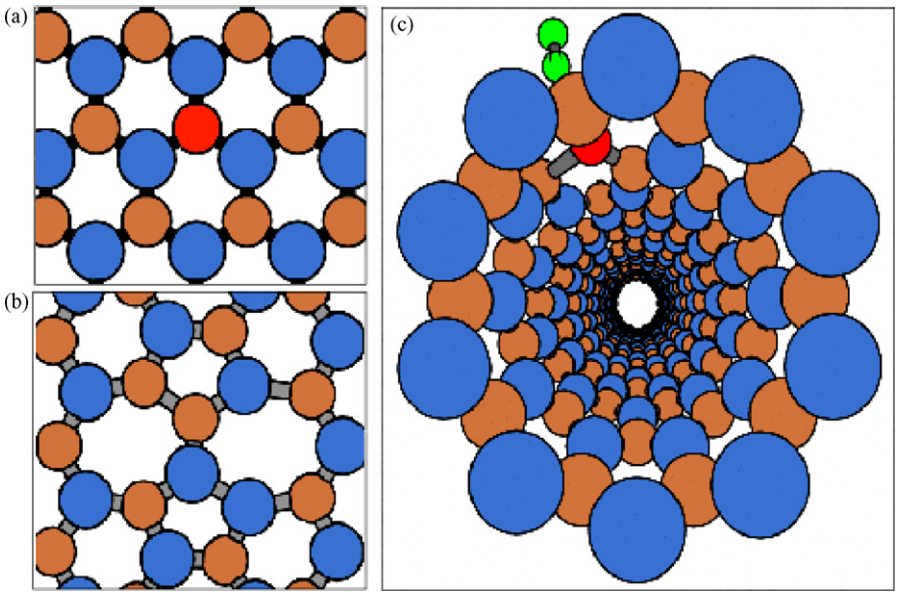

Fig. 2. Schematic drawing of the BNT chemically activated by atomic defects. (a) Atomic substitution in BNT with carbon or oxygen (a red circle), (b) 5 × 7 Stone–Wales defects, and (c) (10,0) boron nitride nanotube with hydrogen (green circles) on top of activated sites. Boron and nitrogen atoms are depicted as blue and dark orange circles in all three figures (for interpretation of the references to color in this figure legend, the reader is referred to the web version of the article).

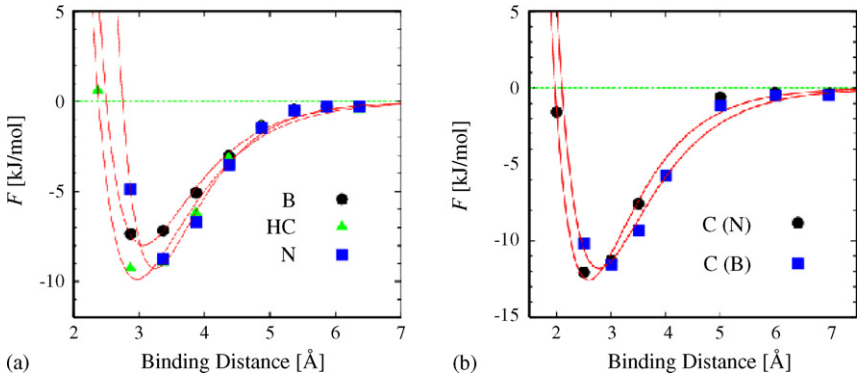

Fig. 3. Binding energy curves of hydrogen: (a) on a perfect (10,0) boron nitride nanotube with hydrogen on top of hexagon center (HC), boron (B), and nitrogen (N), respectively, and (b) on a carbon-doped (10,0) BNT with hydrogen on top of the carbon substituting for boron [C(B)] and for nitrogen [C(N)]. There are about 30% increases of the binding energy near the dopants.

the tubular structure [26]. After structural relaxation, it is found that the bond length of C–B and C–N is 1.53 and 1.41 Å, respectively. The C–N bond length is a little bit smaller than that in a hexagonal carbon nitride and hBN sheet [10,27]. The atomic substitution is found to increase binding energy on BNT by about 30% as shown in Fig. 3(b), which can be translated into a similar increase in T_D. The binding distance is reduced to about 2.95 Å for both substitutions compared to that in the perfect BNT. We note that the enhancement of binding energy is the largest at the top of carbon atom and becomes less significant at other sites. Therefore, a moderate doping rate is necessary to have a global increase of the binding energy. Atomic oxygen is also considered, but it is found that oxygen changes the bonding characteristics of BNT significantly compared to carbon. For oxygen substituting for boron, one of the three O–N bonds is broken at structural relaxation, which indicates that a direct substitutional doping by oxygen may lead to a structural instability of the BNT. Other structural modifications such as 5×7 Stone–Wales defects as shown in Fig. 2(b) are also found to increase the binding energy but their effect is less significant than the chemical doping [10]. The enhancement of binding energy of hydrogen on atomic defects suggests that chemical modifications of sp^2 bonding in BNT can lead to higher binding energies. The local dipole moments at the defect sites may induce a stronger dipole–dipole interaction between hydrogen and the nanotube. Atomic substitution in CNT leads to a similar increase in binding energy, but the enhanced binding energy is smaller than that in perfect and carbon-doped BNTs [21]. For CNT, a somewhat large binding energy is obtained for oxygen-dimer (O_2) substitutional doping of about ~18 kJ/mol. Drastic changes in the bonding tend to increase the hydrogen binding energy, and next we study a more strained chemical modification of the nanotubes.

3.2. Activation through heavy oxygenation of nanotubes

In recent studies, it was found that porous glassy B_2O_3 can have a quite large hydrogen binding energy [9,10]. The enhancement of binding energy was attributed to the pores in

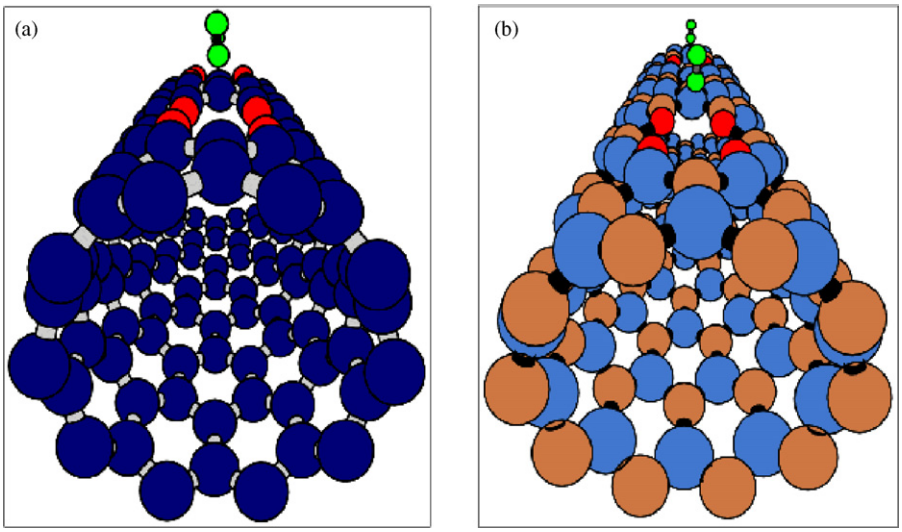

Fig. 4. Schematic drawing of: (a) an (10,0) activated carbon nanotube and (b) an (10,0) activated boron nitride nanotube. The active sites in the activated BNT are created by removing boron (blue) and nitrogen atoms (dark orange) and then substituting neighboring atoms by oxygen atoms (red). The same procedure is also applied for activating CNT (carbon atoms colored in blue). Hydrogen molecule (green) is put on top of the activated sites to calculate its binding energy on the nanotubes (for interpretation of the references to color in this figure legend, the reader is referred to the web version of the article).

B_2O_3, which contain strong ionic B–O bonds and lone-pair electrons from oxygen. We extend this observation to nanotubes and study the effect of chemical activations that mimic the pore structures. The (10,0) zigzag nanotube structure is chosen for both types of nanotubes. Fig. 4 shows a schematic view of an activated: (a) (10,0) carbon and (b) (10,0) boron nitride nanotube studied here, respectively. To emulate the chemical activation that can create similar structures as the pores in B_2O_3, one or two carbon atoms are removed from the nanotubes, and then the atoms neighboring the vacancy are replaced by oxygen atoms. The vacancy–oxygen complexes also resemble the oxygenated edge-structures in activated graphite. The bond length of C–O bonds in the carbon nanotube is obtained to be about 1.38 Å, which is in between the bond length of a single (1.43 Å) and a double C–O bond (1.20 Å). Without hydrogen adsorption, the activated CNT has a radial deformation due to the strain induced by CO bonds. The radial deformation, however, is much reduced when hydrogen binds to the nanotubes. For the activated BNT, the B–O and N–O bond lengths are found to be about 1.38 and 1.46 Å, respectively. The B–O bond length is close to that in B_2O_3 while the N–O bond length is larger than those of both single- and double-bonded N–O.

In order to study the adsorption of hydrogen on such activated nanotubes, a hydrogen molecule is put on top of the sites activated by oxygen. The bond length of hydrogen molecule changes very little upon adsorption. A direct chemical bonding between oxygen and hydrogen atoms is not observed during atomic relaxations, and the reaction barrier for the bonding is estimated to be larger than 1.5 eV. It is interesting to note that there is a small charge transfer from nanotube to hydrogen of about 0.05 electron/H_2 as estimated from the Mulliken population analysis. The charge transfer in the oxygen-activated nanotubes is comparatively larger than that in non-activated nanotubes. This implies that the hydrogen adsorption on activated nanotubes may not be a pure physisorption type. The hydrogen binding energy on the activated nanotubes was calculated to be about 22–29 kJ/mol as shown in Fig. 5. The calculated energy is in a marginal energy range for physisorption. Nonetheless, the increase of the binding energy on top of the activated sites is mostly due to larger contact area for hydrogen binding, which is a signature of physisorption. For the activated CNTs, it was found that the binding distance and energy are correlated: the shorter the binding distance the larger the binding energy. The binding energy is calculated to be about 29 kJ/mol with a binding distance of about 2 Å while it is 20 kJ/mol at 2.5 Å.

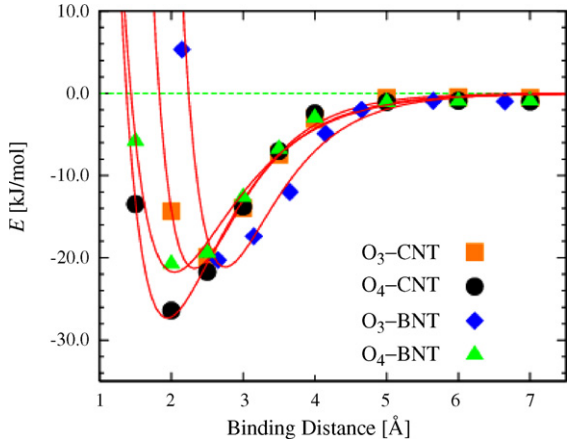

Fig. 5. Binding energy curves of hydrogen on top of activated boron nitride and carbon nanotubes, where the subscript n in O_n-CNT (BNT) is the number of oxygen atoms neighboring the vacancy in the active sites.

The pore size is critical in determining the binding distance and hence the binding energy. Such an effect is found less significant for boron nitride nanotubes. Previous calculations of hydrogen binding on B_2O_3 also showed that the energy depends on the size of the pores on which the hydrogen is adsorbed [11]. The optimal pore size is also estimated for CNT, and details are given below. Calculated binding energies are in a range right enough that the desorption temperature (or operating temperature of hydrogen storages) could reach as high as about 270 K.

Creating such chemically activated nanotubes can be achieved relatively easily. Recent high-resolution transmission electron microscopy images show that vacancies are created and remain stable in graphite [28]. Structural defects including vacancies in nanotube and graphite can be created by high-energy ion or electron bombardment, or from processing conditions [29–32]. Oxygen molecules react with such defects in graphite, which leads to the formation of oxidized pits. A direct substitution of carbon by oxygen is also possible by wet chemistry or ‘‘molecular surgery’’ applied to nanotubes [33]. Little is known about oxidization of BNTs, but similar methods used in CNTs may be applicable to oxygenating BNTs.

3.3. Hydrogen diffusion through pores

Another interesting issue is the diffusion of molecular hydrogen through the pores of the active sites. In order to estimate the optimal (or minimum) size of pores for efficient hydrogen diffusion, the barrier height of the diffusion is calculated on pores of various sizes. The pores are constructed in such a way that carbon and oxygen atoms make a backbone similar to the porous structures in activated nanotubes. The model pore structures are constructed based on macrocyclic polyethers known as crown ethers. It was found that the structure remains quite rigid during structural relaxations. In the present configuration, hydrogen atoms are symmetrically attached to carbon atoms [34]. Therefore, the model molecules have mirror symmetry with respect to the plane containing carbon atoms. The chemical bonding at the pores is almost identical to that in the activated CNT considered here.

Fig. 6 shows the calculated sorption energy curves at varying hydrogen–pore distances. The optimum size of pores was estimated to be about 6 Å, which gives a binding energy of about 30 kJ/mol and a negligible energy barrier for hydrogen diffusion. It is interesting to compare the optimum pore size of 6 Å with that in boron oxides, which have a similar size of pores for efficient hydrogen diffusion [11]. This implies that local chemistries near the binding sites are more critical than the overall compositions of adsorbents for hydrogen binding and

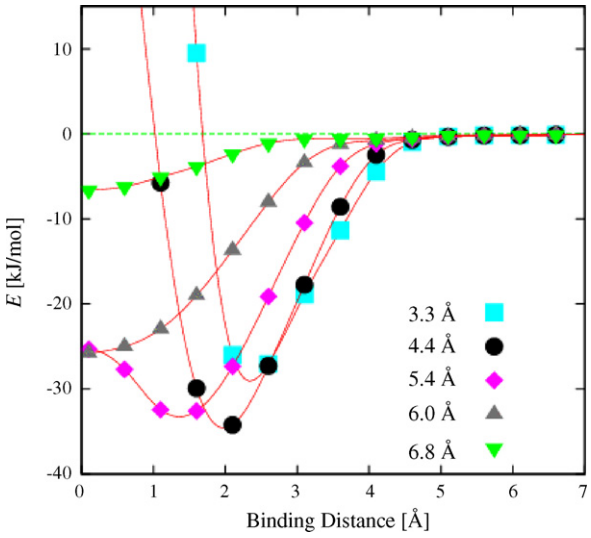

Fig. 6. Calculated binding energy curves of hydrogen on the pores of various sizes. The difference between the energy at the optimum distance, where the energy is lowest, and that at 0 Å is considered as the energy barrier for hydrogen diffusion through the pores.

diffusion. Studies of direct introduction of such large pores into nanotubes are underway.

A heavy oxidization of carbons could also create similar surface chemistries and pore structures for strong hydrogen sorption [35]. With sufficient pores and oxidization as well as high surface area, activated carbons, nanotubes, or polymers could be good candidate media for storing hydrogen near room temperatures, which needs further experimental tests.

4. Conclusions

The hydrogen adsorption on activated boron nitride and carbon nanotubes is studied by quantum mechanical simulations. It is found that the binding energy of hydrogen can reach as high as 29 kJ/mol at activated sites in the nanotubes. Their desorption temperature is estimated to be close to room temperature. This study shows that severe chemical treatments such as peroxidation can lead to a drastic increase of hydrogen binding energy on nanotubes, thus demonstrating a possibility of designing room temperature hydrogen storage based on atomistic simulations.

Acknowledgements

This work was supported by the POSTECH BSRI Research Fund 2005 (Grant No. 1RB0510401) and the Korea Research Foundation Grant funded by the Korea Government (MOEHRD) (KRF-2005-C00041).

References

[1] For an overview, see the DOE Report presented by M. Dresselhaus at DOE Nano Summit, June 2004.
[2] L. Schlapbach, A. Zuttel, Nature 414 (2001) 353.
[3] A. Zuttel, Mater. Today 6 (2003) 24.
[4] J.S. Noh, R.K. Agarwal, J.A. Schwarz, Int. J. Hydrogen Energy 12 (1987) 693;
W.Q. Deng, X. Xu, W.A. Goddard, Phys. Rev. Lett. 92 (2004) 166103;
T. Yildrim, S. Ciraci, Phys. Rev. Lett. 94 (2005) 175501.
[5] M. Rzepka, P. Lamp, M.D.L. Casa-Lillo, J. Phys. Chem. B 102 (1998) 10894.
[6] A. Csaplinski, E. Zielinski, Przem. Chem. 37 (1958) 640.
[7] A. Herbst, P. Harting, Adsorption 8 (2002) 111.
[8] The van't Hoff equation, describing the equilibrium pressure (p) of gas adsorption at temperature (T), is given as $\log(p) = -H/k_BT + \Delta S/R$, where ΔH is the heat of adsorption, k_B Boltzmann constant, ΔS the change in entropy, and R is the gas constant. The desorption temperature is defined as a temperature that gives the equilibrium pressure of 1 atmospheric pressure.
[9] S.-H. Jhi, Y.K. Kwon, K. Bradley, J.C.P. Gabriel, Solid State Commun. 129 (2004) 769.
[10] S.-H. Jhi, Y.K. Kwon, Phys. Rev. B 69 (2004) 245407.
[11] S.-H. Jhi, Y.K. Kwon, Phys. Rev. B 71 (2005) 35408.
[12] X. Blase, A. Rubio, S.G. Louie, M.L. Cohen, Europhys. Lett. 28 (1994) 335.
[13] M. Menon, D. Srivastava, Chem. Phys. Lett. 307 (1999) 407.
[14] M.L. Cohen, Phys. Scr. T1 (1982) 5.
[15] D. SanchezPortal, P. Ordejon, E. Artacho, J.M. Soler, Int. J. Quantum Chem. 65 (1997) 453.
[16] J.P. Perdew, K. Burke, M. Ernzerhof, Phys. Rev. Lett. 77 (1996) 3865.
[17] D.R. Lide (Ed.), Handbook of Chemistry and Physics, 81st ed., CRC Press, New York, 2000/2001.
[18] C.M. Brown, T. Yildirim, D.A. Newmann, M.J. Heben, T. Gennett, A.C. Dillon, J.L. Alleman, J.E. Fischer, Chem. Phys. Lett. 329 (2000) 311.
[19] J.S. Arellano, L.M. Molina, A. Rubio, M.J. L'opez, J.A. Alonso, J. Chem. Phys. 117 (2002) 2281.
[20] Q. Wang, J.K. Johnson, J. Chem. Phys. 110 (1999) 577.
[21] Y.-K. Kwon, S.-H. Jhi, unpublished.
[22] R. Ma, Y. Bando, H. Zhu, T. Sato, C. Xu, D. Wu, J. Am. Chem. Soc. 124 (2002) 7672.
[23] R. Ma, Y. Bando, T. Sato, D. Golberg, H. Zhu, C. Xu, D. Wu, Appl. Phys. Lett. 81 (2002) 5225.
[24] H. Marsh, D. Crawford, T.M. O'Grady, A. Wennerberg, Carbon 20 (1982) 419.
[25] J. Cumings, A. Zettl, Chem. Phys. Lett. 316 (2000) 211.
[26] W.Q. Han, J. Cummings, A. Zettl, Appl. Phys. Lett. 78 (2001) 2769.
[27] A.Y. Liu, M.L. Cohen, Phys. Rev. B 41 (1990) 10727.
[28] A. Hashimoto, K. Suenaga, A. Gloter, K. Urita, S. Iijima, Nature 430 (2004) 870.
[29] P. Ajayan, V. Ravikumar, J.-C. Charlier, Phys. Rev. Lett. 81 (1998) 1437.
[30] Y. Zhu, T. Yi, B. Zheng, L. Cao, Appl. Surf. Sci. 137 (1999) 83.
[31] J. Hahn, H. Kang, S. Lee, Y. Lee, J. Phys. Chem. B 103 (1999) 9944.
[32] C. Kiang, W. Goddard, R. Beyers, D. Bethune, J. Phys. Chem. 100 (1996) 3749.
[33] K. Komatsu, M. Murata, Y. Murata, Science 307 (2005) 238.
[34] S.-H. Jhi, Microporous Mesoporous Mater. 89 (2006) 138.
[35] S.M. Lee, Y.H. Lee, Y.G. Hwang, J.R. Hahn, H. Kang, Phys. Rev. Lett. 82 (1999) 217.